Critical concentration for the doping-induced metal–nonmetal transition in cubic and hexagonal GaN

A. Ferreira da Silva and C. Persson

Citation: J. Appl. Phys. **92**, 2550 (2002); doi: 10.1063/1.1499202
View online: http://dx.doi.org/10.1063/1.1499202
View Table of Contents: http://jap.aip.org/resource/1/JAPIAU/v92/i5
Published by the American Institute of Physics.

Critical concentration for the doping-induced metal–nonmetal transition in cubic and hexagonal GaN

A. Ferreira da Silva[a)]
Instituto de Física, Universidade Federal da Bahia, Campus Universitário de Ondina, 40210 310 Salvador, Bahia, Brazil

C. Persson
Condensed Matter Theory Group, Department of Physics, Uppsala University, Box 530, SE-751 21 Uppsala, Sweden

(Received 5 February 2002; accepted for publication 13 June 2002)

The critical concentration for the metal–nonmetal transition has been calculated for *n*-type and *p*-type GaN. Both cubic and hexagonal structures of GaN have been considered. Three different computational methods have been utilized: the first is the original Mott model, the second is an extended Mott–Hubbard model, and the third method is based on total energy of the metallic and the nonmetallic phases. All three methods show a similar value of the critical concentration, about 10^{18} and 10^{20} cm^{-3} for *n*-type and *p*-type doped materials, respectively. © *2002 American Institute of Physics.* [DOI: 10.1063/1.1499202]

I. INTRODUCTION

The GaN materials are wide-band-gap semiconductors with low compressibility, good thermal stability, and with chemical and radiation inertness.[1,2] Comprehensive investigations of the wurtzite (WZ) structures have led to commercial optoelectronic devices like GaN-based light-emitting diodes and detectors working in the visible–ultraviolet region,[1–3] as well as metal–semiconductor field-effect transistors.[4] Due to the recent progress in crystal growth, one can now also produce thin films of zinc-blende (ZB) GaN,[5,6] which opens up further technological applications. In order to design GaN-based devices properly, it is important to know at which dopant concentration the material transforms from a semiconductor into a metallic state, the so-called metal–nonmetal (MNM) transition or alternatively the Mott transition.[7]

This article describes three different methods for calculating the critical concentration at which the MNM transition occurs. The first two models are based on the probability for the donors to be ionized (describing the transition), whereas the third model is based on a comparison between the total energy before and after the MNM transition (and does thus not describe the actual transition). We present the calculated critical concentration N_c for *n*-type and *p*-type ZB-GaN as well as *n*-type and *p*-type WZ-GaN. Although, we utilize two essentially different types of theories, all three models give fairly similar results. Furthermore, it is shown that N_c is about 1.0×10^{18} cm^{-3} for *n*-type GaN and above 7.0×10^{19} cm^{-3} for *p*-type GaN.

II. COMPUTATIONAL METHODS

All three models are derived within the zero-temperature formalism. The effective-mass approximation is used, and knowledge of the electronic structure of the intrinsic materials is thus required. In the present work, the electronic band structure has been determined from a relativistic, full-potential linearized augmented plane wave method, using the local density approximation in the density functional theory. Further information about the band structure calculation can be found in Refs. 8 and 9. Throughout this article, centimeter-gram-second units have been employed. The three models below are described for *n*-type materials, but the corresponding expressions for *p*-type materials are easily found by treating the holes as particles and the electrons as antiparticles.[10]

A. Model no. 1: Original Mott model

In the original Mott model, the MNM transition occurs at the critical impurity concentration N_c given by[11]

$$N_c \approx \left(\frac{0.25}{a_H^*}\right)^3. \tag{1}$$

Here, a_H^* is the effective Bohr radius. The effective Bohr radius can be calculated from the ionization energy E_D of a single-donor electron

$$a_H^* = \frac{e^2}{2\kappa_0 E_D}, \tag{2}$$

since the donor electron wave function is associated with only one conduction-band maximum, i.e., there are no many-valley effects. In Eq. (2), κ_0 is the static limit of the frequency dependence screening of the host material:[12,13]

$$\frac{1}{\kappa(\omega)} = \frac{1}{\kappa_\infty} - \frac{(\kappa_0-\kappa_\infty)\omega_{\mathrm{LO}}}{2\kappa_0\kappa_\infty}\left(\frac{1}{\omega+\omega_{\mathrm{LO}}-i\delta} - \frac{1}{\omega-\omega_{\mathrm{LO}}+i\delta}\right), \tag{3}$$

a)Electronic mail: ferreira@fis.ufba.br

where δ is an infinitesimal, positive number and ω_{LO} is the frequency of the longitudinal optical (LO) phonons. We have employed experimental values[1] for the lattice dielectric function of WZ-GaN: $\omega_{LO}=92$ meV, $\kappa_0=9.98$, and $\kappa_\infty=5.60$. Calculations of the phonon frequencies by Kim *et al.*[14] are in close agreement with the measured values.[1,15–19] The anisotropy of the dielectric function of the WZ structures has been shown to be small in the materials considered here,[8,15] and we, therefore, use isotropic lattice dielectric functions. Moreover, we assume that the ZB structures have the same lattice dielectric function as the corresponding WZ structures. This assumption is supported by calculations of the optical properties of WZ and ZB III-nitrides in Refs. 20–23, and by spectroscopic ellipsometry measurements of Logothetidis *et al.*[18]

B. Model no. 2: Mott–Hubbard description

Through the use of a Mott–Hubbard tight-binding Hamiltonian, the impurity density of states associated with it present two subbands that overlap with increasing concentration. This would occur at an impurity concentration for which[24–26]

$$\Delta W/U=1.15, \tag{4}$$

where ΔW is the unperturbed impurity bandwidth in units of E_D, and U is the intraimpurity Coulomb interaction energy, also known as the Hubbard-U, given by $U=0.96\cdot E_D$.[27,28] Such a scenario is well known as the Mott–Hubbard picture for the MNM transition. ΔW is related to the hopping integral energy T, between adjacent sites i and j, as[26,27]

$$\Delta W=2|\langle T\rangle|, \tag{5}$$

where $\langle T\rangle$ is defined as the average hopping energy[26,27]

$$\langle T\rangle=\int T(R)P(R)dR. \tag{6}$$

$P(R)$ describes the distribution of the donors. Moreover, $T(R)$ and U are given by[29]

$$T(R)=\int \psi_i(\mathbf{r})\hat{H}_1\psi_j(\mathbf{r}-\mathbf{R}_j)d\mathbf{r},$$

$$U=\int |\psi_1(\mathbf{r}_1)|^2|\psi_2(\mathbf{r}_2)|^2\frac{e^2}{\kappa_0|\mathbf{r}_1-\mathbf{r}_2|}d\mathbf{r}_1d\mathbf{r}_2. \tag{7}$$

$\hat{H}_1$ is the one-particle Hamiltonian in the effective-mass theory, including the kinetic energy operator and the Coulomb interaction of the positively charged donor ion and the electron. $\psi_j(\mathbf{r}-\mathbf{R}_j)$ is the simple hydrogenic wave function for the donor ground state at the randomly located site $\mathbf{R}_j$. Moreover, we have used a randomlike Poisson distribution $P(R)$ of the donors with the probability that the nearest donor neighbor lies at a distance R (in units of a_H^*):

$$P(R)=\frac{3R^2}{R_D^3}\left(1+\frac{R^2}{R_D^3}\right)^{-1}, \quad \text{where}$$

$$R_D=\left(\frac{4\pi N_D}{3}\right)^{-1/3}. \tag{8}$$

Equations (5) to (8) show that the values of U and the donor impurity concentration N_D are both related to the ionization energy E_D. Using these equations, we have calculated the values of the critical concentration N_c. The transition is obtained by Eq. (4).

C. Model no. 3: Total energy approach

The third model follows a method expounded by Sernelius and Berggren,[13] where the total energy E_{tot}^{NM} of the localized donor electrons in the nonmetallic phase is determined and compared with the total energy E_{tot}^{M} of the electron gas in the metallic phase. For low donor concentrations, the total energy of the localized electrons is lower than the corresponding energy of the electron gas, and thus the nonmetallic phase is favored. For high donor concentrations the situation is the reversed, unless the ionization energy is not too large. The critical concentration for the transition can be estimated as the concentration at which the total energies of the two phases are equal, i.e., $E_{tot}^{NM}=E_{tot}^{M}$.

The total energy for the nonmetallic phase is directly related to the dielectric function of the localized electrons associated with the donors. Leroux Hugon and Ghazali[30] have derived the dielectric function of the donor electrons as a function of impurity concentration, where a hydrogenic wave function was presumed. When the concentration is increased, the donor electrons screen the Coulomb potential of the impurities more strongly, whereby the dielectric function is increased. The change in the dielectric function will modify the ionization energy of the electrons, and thereby also the total energy. The total energy (expressed in energy per electrons) of the donor electrons in the nonmetallic phase is obtained as[13,31]

$$E_{tot}^{NM}=-E_D\cdot\left(\frac{1}{2}+\frac{(0.21/a_H^*)^3}{3N_D}\times\left[1-\left(1-\frac{N_D}{(0.21/a_H^*)^3}\right)^{3/2}\right]\right). \tag{9}$$

The total energy of the electron gas in the metallic phase has been calculated using a many-particle Green's function formalism. The total energy can be divided into the kinetic energy E_{kin}, the exchange–correlation energy E_{xc}, and the energy from the electron–ion interaction E_{ion} caused by electron relaxation near the donor ions. Since lattice vibrations are not taken into account in the intrinsic band structure, one also has to included the polaron energy E_p, describing the interaction between the electrons and the optical phonons. The total energy is thus: $E_{tot}^{M}=E_{kin}+E_{xc}+E_{ion}+E_p$.

The kinetic energy (per electron) of a noninteracting electron gas is given by

$$E_{kin}=\frac{2}{n}\sum_j\int\frac{d\mathbf{k}}{(2\pi)^3}E_j^0(\mathbf{k})\,\eta_j(\mathbf{k}), \tag{10}$$

where $n=N_D$ is the electron concentration, and $\eta_j(\mathbf{k})$ is one (zero) if the $\mathbf{k}$ state in the jth band is occupied (not occupied) by an electron. The summation runs over all λ conduction bands which are populated by the electron gas ($\lambda=1$ for n-type GaN).

The exchange and the correlation contributions to the total energy are directly related to the (testparticle–particle) dielectric function $\tilde{\epsilon}(\mathbf{q},\omega)$, describing the response of the electron gas to perturbations in the electron distribution.[12,32] We have calculated the dielectric function according to the random phase approximation with an average local-field correction of Hubbard:[13,31,33,34]

$$\tilde{\epsilon}(\mathbf{q},\omega)=1+[1-(\overline{f}(\mathbf{q})/\lambda)]\alpha^0(\mathbf{q},\omega)$$
$$\overline{f}(\mathbf{q})=\frac{1}{2\lambda}\sum_j \frac{E_j^0(\mathbf{q})}{E_j^0(\mathbf{q})+E_F^0}, \tag{11}$$

where E_F^0 is the Fermi energy of the electron gas. The polarizability $\alpha^0(\mathbf{q},\omega)$ is defined as[12,32–35]

$$\alpha^0(\mathbf{q},\omega)=\frac{-2v(\mathbf{q})}{\hbar\kappa(\omega)}\int\frac{d\mathbf{k}}{(2\pi)^3}\int_{-\infty}^{\infty}\frac{d\omega'}{2\pi i}\sum_j G_j^0(\mathbf{k},\omega')$$
$$\times G_j^0(\mathbf{k}+\mathbf{q},\omega'+\omega), \tag{12}$$

neglecting intervalley scattering. $G_j^0(\mathbf{k},\omega)$ is the Green's function for noninteracting particles:

$$G_j^0(\mathbf{k},\omega)=\frac{\eta_j(\mathbf{k})}{\omega-E_j^0(\mathbf{k})/\hbar-i\delta}+\frac{1-\eta_j(\mathbf{k})}{\omega-E_j^0(\mathbf{k})/\hbar+i\delta}. \tag{13}$$

The exchange–correlation energy of an electron gas is[13,31,32]

$$E_{\mathrm{xc}}=\frac{\hbar}{2n}\int\frac{d\mathbf{q}}{(2\pi)^3}\int_{-\infty}^{\infty}\frac{d\omega}{2\pi i}\left\{\frac{\ln(\tilde{\epsilon}(\mathbf{q},\omega))}{1-\overline{f}(\mathbf{q})/\lambda}\right.$$
$$-\frac{v(\mathbf{q})}{\kappa(\omega)}\frac{2}{\hbar}\int\frac{d\mathbf{k}}{(2\pi)^3}$$
$$\times\sum_j\left(\frac{\eta_j(\mathbf{k})}{\omega+[E_j^0(\mathbf{k}+\mathbf{q})-E_j^0(\mathbf{k})]/\hbar-i\delta}\right.$$
$$\left.\left.-\frac{\eta_j(\mathbf{k})}{\omega-[E_j^0(\mathbf{k}+\mathbf{q})-E_j^0(\mathbf{k})]/\hbar+i\delta}\right)\right\}, \tag{14}$$

where the second term is the electrostatic self-interaction energy of the electrons.

The relaxation of the electrons around the donor ions is taken into account through the electron–ion interaction. This is mainly a correlation contribution, describing the difference in the electron density between a system with uniform distribution of the donor–ion charges and a system with point-like ions. In the second-order perturbation theory the electron–ion energy is given by[13,31,32]

$$E_{\mathrm{ion}}=\frac{-N_D}{2n}\int\frac{d\mathbf{q}}{(2\pi)^3}\frac{v(\mathbf{q})}{\kappa_0}\cdot\frac{\alpha^0(\mathbf{q},0)}{\tilde{\epsilon}(\mathbf{q},0)}, \tag{15}$$

TABLE I. The critical concentration N_c for the MNM transition for different *n*-type and *p*-type GaN materials with different donor (E_D) or acceptor (E_A) ionization energies. Three calculations models have been employed: the Mott model, an extended Mott–Hubbard model, and a total energy model based on a many-particle Green's function formalism.

			N_c cm^{-3}			
	Dopant	$E_{D,A}$ (meV)	Mott	Mott–Hubbard	Total energy	Ref. 37
n-type						
ZB-GaN		25[a,b]	6.5×10^{17}	5.3×10^{17}	4.9×10^{17}	
		32[c,d]	1.4×10^{18}	1.1×10^{18}	1.4×10^{18}	
WZ-GaN	Si	30[e,f]	1.1×10^{18}	9.1×10^{17}	7.0×10^{17}	$\sim1.0\times10^{18}$
	O	33[e]	1.5×10^{18}	1.2×10^{18}	1.0×10^{18}	
	O	34[g,h]	1.6×10^{18}	1.3×10^{18}	1.2×10^{18}	
p-type						
ZB-GaN		130[b]	9.1×10^{19}	7.4×10^{19}	2.8×10^{19}	
		166[i]	1.9×10^{20}	1.5×10^{20}	6.8×10^{19}	
	C	215[a]	4.1×10^{20}	3.3×10^{20}	1.7×10^{20}	
	Mg	230[a,j,k]	5.0×10^{20}	4.1×10^{20}	2.2×10^{20}	
WZ-GaN	Si	203[l]	3.5×10^{20}	2.8×10^{20}	1.8×10^{20}	
	Mg	209[g]	3.8×10^{20}	3.1×10^{20}	2.1×10^{20}	
	O	230[l,m]	5.0×10^{20}	4.1×10^{20}	3.0×10^{20}	
	Mg	250[k,n]	6.4×10^{20}	5.2×10^{20}	4.1×10^{20}	

[a]See Ref. 38.
[b]See Ref. 39.
[c]See Ref. 40.
[d]See Ref. 41.
[e]See Ref. 42.
[f]See Ref. 43.
[g]See Ref. 44.
[h]See Ref. 45.
[i]See Ref. 46.
[j]See Ref. 47.
[k]See Ref. 48.
[l]See Ref. 49.
[m]See Ref. 50.
[n]See Ref. 1.

presuming that the donors are randomly distributed and have infinitely large masses.

Finally, in ionic materials there is also an additional contribution from the electron optical phonon interaction:[12,31,32]

$$E_p=\frac{\hbar}{2n}\int\frac{d\mathbf{q}}{(2\pi)^3}\int_{-\infty}^{\infty}\frac{d\omega}{2\pi i}\left(\frac{v(\mathbf{q})}{\kappa(\omega)}+\frac{v(\mathbf{q})}{\kappa_\infty}\right)\frac{2}{\hbar}\int\frac{d\mathbf{k}}{(2\pi)^3}\times\sum_j\left(\frac{\eta_j(\mathbf{k})}{\omega+[E_j^0(\mathbf{k}+\mathbf{q})-E_j^0(\mathbf{k})]/\hbar-i\delta}-\frac{\eta_j(\mathbf{k})}{\omega-[E_j^0(\mathbf{k}+\mathbf{q})-E_j^0(\mathbf{k})]/\hbar+i\delta}\right)+\frac{e^2}{2}\sqrt{\frac{2m_d}{\hbar^3\omega_{\mathrm{LO}}}}\left(\frac{1}{\kappa_\infty}-\frac{1}{\kappa_0}\right)\hbar\omega_{\mathrm{LO}}. \quad (16)$$

This polaron energy is independent of impurity concentration, and can be seen as a modification of the electrostatic self-interaction in the intrinsic crystal.

These equations are for *n*-type materials with parabolic conduction-band minimum. Corresponding expressions hold for *p*-type doped materials. However, since the uppermost valence bands are very nonparabolic in the vicinity of the Γ point, we have used dopant dependent effective hole masses in the case of *p*-type materials. The masses are chosen in such way that the Fermi energy for the parabolic bands always coincides with the Fermi energy obtained by using the numerical energy dispersion from a band structure calculation. This approximation and the used effective hole masses are rigorously described in Refs. 35 and 36.

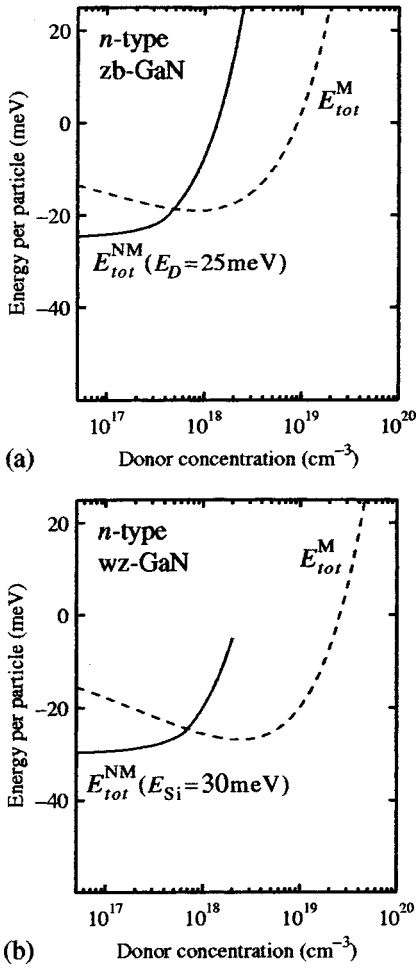

FIG. 1. Total energies per particle of the metallic E_{tot}^{M} (dashed line) and the nonmetallic $E_{\mathrm{tot}}^{\mathrm{NM}}$ (solid line) phases in *n*-type GaN as functions of dopant concentration, obtained from Eqs. (9)–(16).

III. RESULTS

The calculated critical concentrations for MNM transition in *n*-type and *p*-type ZB-GaN as well as in *n*-type and *p*-type WZ-GaN are presented in Table I. There are two model calculations for the ionization energies of *n*-type WZ- and ZB-GaN,[41,42] and many discussions about their values obtained experimentally.[1,37–40,42,44,45,48–51] The values obtained for Si, O, and C levels lead to $E_{\mathrm{Si}}<E_{\mathrm{O}}<E_{\mathrm{C}}$. Moreover, Moore *et al.*[42] have recently claimed to find an unidentified donor level, E_{uni}, in WZ-GaN which leads to $E_{\mathrm{Si}}<E_{\mathrm{uni}}<E_{\mathrm{O}}$, or 30.2 meV$<$31.2 meV$<$33.2 meV. We use in the calculation the values obtained experimentally, which are in the range of 25–34 meV.[38–40,42] Götz *et al.*[44] with a Hall measurement have found a metallic regime for *n*-type WZ-GaN in a range of $7.0\times10^{17}<N_c<2.0\times10^{19}$ cm^{-3}. The nature of the involved shallow donor and acceptor in ZB-GaN has not yet been identified clearly, but As *et al.*[38,47] have identified C and Mg as acceptors.

From Table I, one can notice that the extended Mott–Hubbard model gives a slightly smaller N_c that the original Mott model for the materials considered here. Furthermore, the method based on the total energy results in even lower critical concentrations, except for *n*-type ZB-GaN with $E_D=32$ meV. But the three computational methods give the same order of N_c, although two of the models are derived by using rather different approaches.

In the Mott model, the critical concentration is proportional to E_D^3. The same relation holds, with fairly good accuracy, also in the Mott–Hubbard model. For the total energy calculation, however, this is not longer true, especially not for large ionization energies. For sufficiently large ionization energy (estimated to be 50–100 meV in *n*-type GaN), the total energies per particle in the metallic E_{tot}^{M} and in the nonmetallic $E_{\mathrm{tot}}^{\mathrm{NM}}$ phases do not become equal at any concentration since the average kinetic energy of the free electron gas (in the single conduction band) is too high, which implies too large screening for a transition. That can be seen in Fig. 1, where we show E_{tot}^{M} and $E_{\mathrm{tot}}^{\mathrm{NM}}$ of *n*-type GaN. For high donor concentrations, E_{tot}^{M} is increasing drastically due to large kinetic energy of the electrons in the electron gas (the large kinetic energy is directly related to the small effective electron mass of the single conduction-band minimum). For *p*-type GaN, as presented in Fig. 2, the flat band structure the valence-band maximum (consisting of three valence bands) results in relatively low kinetic energies of the hole gas also at high hole concentrations. Hence, the transition in *p*-type GaN can occur at relatively high acceptor concentrations. However, the resulting critical concentrations for *p*-type GaN are high for Mg as acceptor in WZ-GaN (with large ioniza-

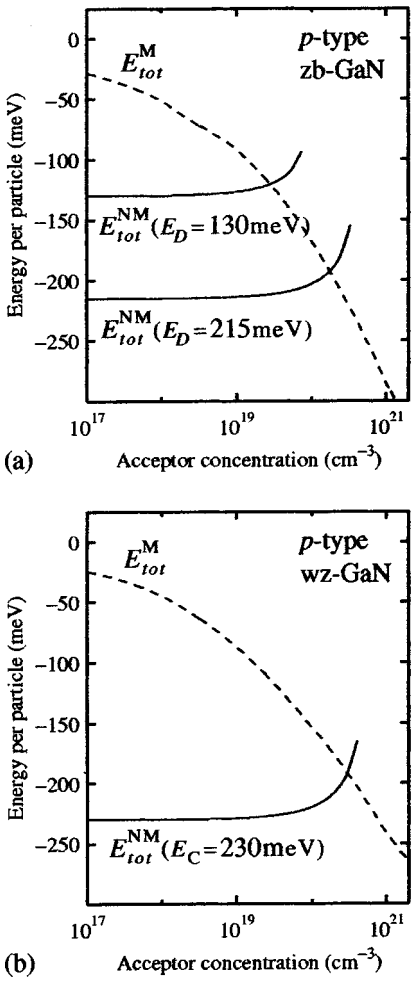

FIG. 2. Same as Fig. 1, but for *p*-type doping.

tion energies) and N_c is near the upper limit to the dopant concentrations of interest in devices.

IV. SUMMARY AND DISCUSSION

In conclusion, the critical concentration for the MNM transition has been calculated for different *n*-type and *p*-type GaN, considering both cubic and hexagonal structures and utilizing three different computational models. We have shown that the three models give similar results.

The Mott–Hubbard model describes the actual MNM transition in terms of the intraimpurity Coulomb interaction and the hopping integral, whereas the total energy calculation describes the low-concentration and high-concentration phases. Although the Mott–Hubbard (and the original Mott) model and the total energy model have different approaches to describe the transition, the three computational methods give the same order of N_c. The first two methods, namely Mott and Mott–Hubbard, do not depend on the structure of the material. The third method, based on total energies of the metallic and nonmetallic phases, depends on the structure of the considered material, i.e., WZ or ZB, as was described in the text. In Table I, we can see this difference for ZB-GaN:Mg and WZ-GaN:O, which have the same ionization energies. This type of impurity atom does not affect the two first model calculations since the donor electrons are treated as hydrogenlike wave functions. The main reason for the high values of N_c in *p*-type GaN originates from the large ionization energies.

It is worth mentioning that the reliability of the Mott–Hubbard approach, expressed by Eq. (4), is very well discussed in Refs. 52–55 in terms of two different Hubbard bands touching each other, leading to the MNM transition. The total energy approach has been described for *n*-type materials in Refs. 13 and 31.

ACKNOWLEDGMENTS

This work was financially supported by the Brazilian National Research Council (CNPq) and the Swedish Research Council.

[1] S. Strite and H. Morkoc, J. Vac. Sci. Technol. B **10**, 1237 (1992).
[2] S. C. Jain, M. Willander, J. Narayan, and R. Van Overstraeten, J. Appl. Phys. **87**, 965 (2000).
[3] S. Nakamura, M. Senoh, N. Iwasa, S. Nagahama, T. Yamada, and T. Mukai, Jpn. J. Appl. Phys., Part 2 **34**, L1332 (1995).
[4] M. A. Khan, J. N. Kuznia, A. R. Bhattarai, and D. T. Olson, Appl. Phys. Lett. **62**, 1786 (1993).
[5] O. Brandt, *Group III Nitride Semiconductor Compounds*, edited by B. Gil (Clarendon, Oxford, 1998).
[6] D. Schikora, M. Hankeln, D. J. As, K. Lischka, T. Litz, A. Waag, T. Buhrow, and F. Henneberger, Phys. Rev. B **54**, 8381 (1996).
[7] N. F. Mott and E. A. Davis, *Electronic Processes in Noncrystalline Materials*, 2nd ed. (Clarendon, Oxford, 1979).
[8] C. Persson, A. Ferreira da Silva, R. Ahuja, and B. Johansson, J. Cryst. Growth **231**, 397 (2001).
[9] C. Persson, Bo E. Sernelius, A. Ferreira da Silva, R. Ahuja, and B. Johansson, J. Phys.: Condens. Matter **13**, 8915 (2001).
[10] C. Persson, A. Ferreira da Silva, and B. Johansson, Phys. Rev. B **63**, 205119 (2001).
[11] N. F. Mott, Can. J. Phys. **34**, 1356 (1956).
[12] G. D. Mahan, *Many-Particle Physics*, 2nd ed. (Plenum, New York, 1990).
[13] B. E. Sernelius and K.-F. Berggren, Philos. Mag. B **43**, 115 (1981).
[14] K. Kim, W. R. L. Lambrecht, and B. Segall, Phys. Rev. B **53**, 16310 (1996).
[15] R. Goldhahn, S. Shokhovets, J. Scheiner, G. Gobsch, T. S. Cheng, C. T. Foxon, U. Kaiser, G. D. Kipshidze, and W. Richter, Phys. Status Solidi A **177**, 107 (2000).
[16] G. Brockt and H. Lakner, Micron **31**, 435 (2000).
[17] L. X. Benedict, T. Wethkamp, K. Wilmers, C. Cobet, N. Esser, E. L. Shirley, W. Richter, and M. Cardona, Solid State Commun. **112**, 129 (1999).
[18] S. Logothetidis, J. Petalas, M. Cardona, and T. D. Moustakas, Phys. Rev. B **50**, 18017 (1994).
[19] T. Kawashima, H. Yoshikawa, S. Adachi, S. Fuke, and K. Ohtsuka, J. Appl. Phys. **82**, 3528 (1997).
[20] S.-H. Park and S.-L. Chuang, J. Appl. Phys. **87**, 353 (2000).
[21] C. Persson, R. Ahuja, A. Ferreira da Silva, and B. Johansson, J. Cryst. Growth **231**, 407 (2001).
[22] K. Karch, J.-M. Wagner, and F. Bechstedt, Phys. Rev. B **57**, 7043 (1998).
[23] J.-M. Wagner and F. Bechstedt, Phys. Rev. B **62**, 4526 (2000).
[24] K.-F. Berggren, Philos. Mag. B **27**, 1027 (1973).
[25] P. P. Edwards and M. J. Sienko, Phys. Rev. B **17**, 2575 (1978).
[26] P. Nubile and A. Ferreira da Silva, Solid-State Electron. **41**, 121 (1997).
[27] A. Ferreira da Silva, J. Appl. Phys. **76**, 5249 (1994).
[28] E. Abramof, A. Ferreira da Silva, B. E. Sernelius, J. P. de Souza, and H. Boudinov, J. Mater. Res. **12**, 641 (1997).
[29] A. Ferreira da Silva, Phys. Scr., T **14**, 27 (1986).
[30] P. Leroux Hugon and A. Ghazali, Phys. Rev. B **14**, 602 (1976).
[31] C. Persson, U. Lindefelt, and B. E. Sernelius, Phys. Rev. B **60**, 16479 (1999).
[32] B. E. Sernelius, Phys. Rev. B **34**, 5610 (1986).
[33] J. Hubbard, Proc. R. Soc. London, Ser. A **243**, 336 (1957).
[34] A. A. Kugler, J. Stat. Phys. **12**, 35 (1975).
[35] C. Persson, U. Lindefelt, and B. E. Sernelius, J. Appl. Phys. **86**, 4419 (1999).

[36] C. Persson, B. E. Sernelius, A. Ferreira da Silva, R. Ahuja, and B. Johansson (unpublished).
[37] A. Ferreira da Silva, C. Moysés Araújo, Bo E. Sernelius, C. Persson, R. Ahuja, and B. Johansson, J. Phys.: Condens. Matter **13**, 8891 (2001).
[38] D. J. As and U. Köhler, J. Phys.: Condens. Matter **13**, 8923 (2001).
[39] D. J. As, F. Schmilgus, C. Wang, B. Schttker, D. Schikora, and K. Lischka, Appl. Phys. Lett. **70**, 1311 (1997).
[40] M. Ramsteiner, J. Menninger, O. Brandt, H. Yang, and K. H. Ploog, Appl. Phys. Lett. **69**, 1276 (1996).
[41] H. Wang and A. B. Chen, J. Appl. Phys. **87**, 7859 (2000).
[42] W. J. Moore, J. A. Freitas, Jr., G. C. B. Braga, R. J. Molnar, S. K. Lee, K. Y. Lee, and I. J. Song, Appl. Phys. Lett. **79**, 2570 (2001).
[43] F. Mireles and S. E. Ulloa, Appl. Phys. Lett. **74**, 248 (1999).
[44] W. Götz, N. M. Johnson, C. Chen, H. Liu, C. Kuo, and W. Imler, Appl. Phys. Lett. **68**, 3144 (1996).
[45] W. J. Moore, J. A. Freitas, Jr., and R. J. Molnar, Phys. Rev. B **56**, 12073 (1997).
[46] J. R. L. Fernandez, V. A. Chitta, E. Abramof, A. Ferreira da Silva, J. R. Leite, A. Tabata, D. J. As, T. Frey, D. Schikora, and K. Lischka, MRS Internet J. Nitride Semicond. Res. **595**, W3-40 (2000).
[47] D. J. As, T. Simonsmeier, B. Schöttker, T. Frey, D. Schikora, W. Kriegseis, W. Burkhardt, and B. K. Meyer, Appl. Phys. Lett. **73**, 1835 (1998).
[48] J. Neugebauer and C. G. Van de Walle, Mater. Res. Soc. Symp. Proc. **395**, 645 (1996).
[49] F. Mireles and S. E. Ulloa, Phys. Rev. B **58**, 3879 (1998).
[50] S. Fischer, C. Wetzel, E. E. Haller, and B. K. Meyer, Appl. Phys. Lett. **67**, 1298 (1995).
[51] B. K. Meyer, D. Volm, A. Graber, H. C. Alt, T. Detchprohm, A Mano, and I. Akasaki, Solid State Commun. **95**, 597 (1995).
[52] J. Hubbard, Proc. R. Soc. London, Ser. A **281**, 401 (1964).
[53] N. F. Mott, *Metal–Insulator Transition* (Taylor and Francis, London, 1974).
[54] H. Aoki and H. Kamimura, J. Phys. Soc. Jpn. **40**, 6 (1976).
[55] H. Kamimura, in *The Metal Non-Metal Transition in Disordered Systems*, edited by L. R. Friedman and D. P. Tunstall, Proceedings of the 19th Scottish Universities Summer School in Physics (University of Edinburgh, 1978).